

Chaotic Seismic Torsional Pounding between two Single-story Asymmetric Towers

L.X. Wang¹ and K.T. Chau²

¹ Assistant Professor, Earthquake Administration of Guangdong Province, Guangzhou, China

² Professor, Dept. of Civil and Structural Engineering, The Hong Kong Polytechnic University, Hong Kong, China

Email: wxustc@hotmail.com, cektchau@polyu.edu.hk

ABSTRACT:

Adjacent buildings are subjected to pounding hazard during earthquakes when there are inadequate separation distances. Pounding phenomena have been observed during past major earthquakes, including recent M8.0 Wenchuan Earthquake on May 12, 2008, and have been identified as one of the main causes of structural damages of buildings. However, most of actual poundings are likely to be eccentric due to asymmetric structural plans or non-constant gaps between adjacent buildings. Seismic torsional pounding is a highly nonlinear phenomenon in nature. In this study, the nonlinear Hertz contact law was adopted to simulate impacts between two single-story asymmetric towers. The numerical simulation results show that torsional pounding tends to be much more complex than translational pounding, and most of torsional impacts are chaotic. Group periodic pounding (i.e. a group of non-periodic impacts repeating themselves periodically) observed in shaking table tests by Chau et al. (2003) was replicated numerically for the first time by incorporating torsional responses, which cannot be explained in numerical simulations for translational pounding alone.

KEYWORDS:

Seismic pounding, Torsion, Chaotic, Numerical simulation

1. INTRODUCTION

Seismic pounding (i.e. earthquake induced collisions between adjacent structures) has been frequently observed in past strong earthquakes, for example, in the 1964 Alaska earthquake (Anagnostopoulos 1994), the 1968 Tokachi-Oki earthquake (Wakabayashi 1986), the 1976 Tangshan earthquake (Liu et al. 1993), the 1985 Mexico City earthquake (Rosenblueth and Meli 1986), the 1989 Loma Prieta earthquake (Kasai and Maison, 1997), and the 1999 Chi-Chi earthquake (Naeim et al. 2000). Figure 1 shows two examples of pounding induced damages in the recent massive M8.0 Wenchuan earthquake on May 12, 2008. During the 1989 Loma Prieta earthquake, there were over 200 pounding occurrences involving more than 500 buildings in San Francisco, Oakland, Santa Cruz, and Watsonville (Kasai and Maison, 1997).

A large number of studies have been conducted on modeling seismic pounding between adjacent structures (e.g. Miller 1980; Anagnostopoulos 1988; Jing and Young 1991; Davis 1992; Chau and Wei 2001; Jankowski 2005; Muthukumar and DesRoches 2006). Among them, the pounding models which utilize the nonlinear Hertz contact law (Davis 1992; Chau and Wei 2001; Muthukumar and DesRoches 2006) appear to be more realistic, since structural poundings during earthquakes are seldom linear. However, most of these studies assume a two-dimensional behavior, i.e. only translational pounding is considered. Actually as argued by Leibovich et al. (1996), torsional pounding tends to be more common than unidirectional pounding during real earthquakes, which may be resulted from rotational responses of asymmetric buildings or nonparallel gaps between adjacent structures. For torsional pounding, Leibovich et al. (1996) studied possible eccentric pounding between two symmetric single-story structures; Papadrakakis et al. (1996) developed a three-dimensional finite element model to simulate pounding between adjacent buildings using the Lagrange multiplier method; Mouzakis and Papadrakakis (2004) investigated the three-dimensional pounding between two adjacent buildings based on the impulse-momentum relation; Gong and Hao (2005) studied the torsional pounding between an asymmetric and a symmetric one-storey system subjected to bi-directional ground motion.



Figure 1 Damages caused by pounding during the M8.0 Wenchuan earthquake on May 12, 2008

However, little research has been conducted to adopt the more realistic Hertz contact law to model torsional pounding between asymmetric structures. This paper will extend the models of Davis (1992) and Chau and Wei (2001) to consider the torsional pounding between two adjacent asymmetrical single-story structures using the nonlinear Hertz contact law. The resulting differential equations will be numerically solved using the fourth-order Runge-Kutta method with error control. The effects of various input parameters on torsional pounding will be investigated through numerical simulations.

2. FORMULATION AND NUMERICAL SOLVING

2.1 Equations of Motions

As shown in Figure 2, two rectangular single-story towers (Tower A and Tower B) of equal height and separated by a distance of a' are considered in this study. Each tower is supported by four identical square columns at its four corners. For simplicity, the dimensions of the two towers are assumed to be equal (i.e. $l'_A = l'_B = l'$ and $w'_A = w'_B = w$). Since the four supporting columns are identical and symmetrically distributed, the center of stiffness (denoted by 'CS' in the figure) coincides with the geometric center of each tower. The position of the center of mass (denoted by 'CM' in the figure) is assumed to be a variable. The eccentricities between CM and CS are denoted by e'_{ix}, e'_{iy} ($i = A, B$) along the x and y directions respectively. Without loss of generality, only eccentricity along the y direction and ground motion along the x direction are considered in the present study (i.e. $e'_{Ax} = e'_{Bx} = 0$). In addition, the tower slabs are assumed to be rigid in their own planes and frictionless contact is assumed. The present formulation provides the simplest analytical model incorporating seismic torsional poundings, we believe this study should provide valuable insights into this unknown complex phenomenon.

The motion of each tower is described by three degrees of freedom, that is, two translational displacements along the x and y directions, $u_i(\tau)$ and $v_i(\tau)$, and one rotation about CM, $\theta_i(\tau)$ ($i = A, B$), where τ is the time. The equations of motions of each tower can be written in a matrix form as:

$$\begin{bmatrix} m_i & 0 & 0 \\ 0 & m_i & 0 \\ 0 & 0 & I'_i \end{bmatrix} \begin{Bmatrix} \ddot{u}_i \\ \ddot{v}_i \\ \ddot{\theta}_i \end{Bmatrix} + \begin{bmatrix} c_i & 0 & 0 \\ 0 & c_i & 0 \\ 0 & 0 & c'_i \end{bmatrix} \begin{Bmatrix} \dot{u}_i - \dot{u}_g \\ \dot{v}_i \\ \dot{\theta}_i \end{Bmatrix} + \mathbf{K}_i \begin{Bmatrix} u_i - u_g + \Delta_i \\ v_i - e_{iy} \\ \theta_i \end{Bmatrix} = \begin{Bmatrix} F'_{ix} \\ F'_{iy} \\ T'_{i\theta} \end{Bmatrix} \quad (i = A, B) \quad (2.1)$$

where m_i is the lumped mass, I'_i is the moment of inertia of each tower about a vertical axis through its center of mass, c_i and c'_i denote the translational and torsional damping respectively, F'_{ix} and F'_{iy} are the pounding forces acting on each tower along the x and y directions respectively, $T'_{i\theta}$ is the torque caused by

pounding, and $u_g(\tau) = A_g \sin \omega \tau$ is the ground motion, where A_g and ω are the amplitude and the circular frequency respectively. The matrix \mathbf{K}_i is the stiffness matrix of each tower. For the model shown in Figure 1, it has the following form:

$$\mathbf{K}_i = \begin{bmatrix} 4k_i & 0 & 4k_i e'_{iy} \\ 0 & 4k_i & -4k_i e'_{ix} \\ 4k_i e'_{iy} & -4k_i e'_{ix} & [l_i'^2 + w_i'^2 + 4(e_{iy}'^2 + e_{ix}'^2)]k_i \end{bmatrix} \quad (i = A, B) \quad (2.2)$$

where k_i is the lateral stiffness of each supporting column of the i^{th} tower. For simplicity, all of the columns of the two towers are assumed to be identical (i.e. $k_A = k_B = k$). Thus, if we define K_A and K_B are the lateral stiffness of the two towers, we have $K_A = K_B = 4k$. The other two parameters Δ'_i ($i = A, B$) in Eqn. 2.1 have the forms of $\Delta'_A = \frac{a'}{2} + (\frac{w'_A}{2} - e'_{Ax})$ and $\Delta'_B = -\frac{a'}{2} - (\frac{w'_B}{2} - e'_{Bx})$.

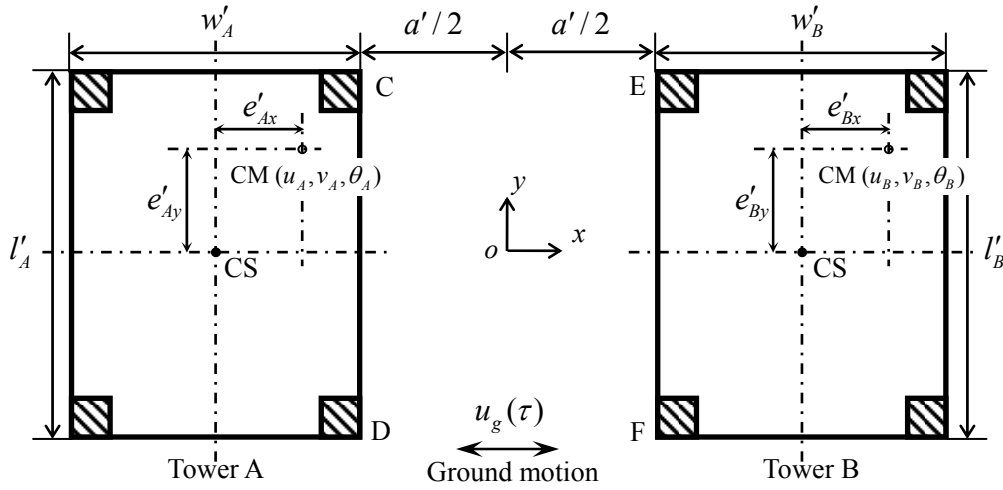


Figure 2 Sketch of two asymmetric rectangular towers separated by a distance a'

If we normalize the dimensions with the excitation amplitude (A_g) as $x_i = u_i / A_g$, $y_i = v_i / A_g$ ($i = A, B$) and normalize the time with the translational natural frequency (ω_{Ax}) of Tower A as $t = \tau \omega_{Ax}$, Eqn. 2.1 can be written in a dimensionless form for Tower A and Tower B as:

$$\begin{Bmatrix} \ddot{x}_A \\ \ddot{y}_A \\ \ddot{\theta}_A \end{Bmatrix} + \begin{bmatrix} 2\zeta_{Ax} & 0 & 0 \\ 0 & 2\zeta_{Ay} & 0 \\ 0 & 0 & 2\zeta_{A\theta} \end{bmatrix} \begin{Bmatrix} \dot{x}_A - \frac{1}{p_1} \cos \frac{t}{p_1} \\ \dot{y}_A \\ \dot{\theta}_A \end{Bmatrix} + \begin{bmatrix} 1 & 0 & e_{Ay} \\ 0 & 1 & -e_{Ax} \\ e_{Ay} \frac{m_A}{I_A} & -e_{Ax} \frac{m_A}{I_A} & \left(\frac{p_3}{p_1}\right)^2 \end{bmatrix} \begin{Bmatrix} x_A - \sin \frac{t}{p_1} + \Delta_A \\ y_A - e_{Ay} \\ \theta_A \end{Bmatrix} = \begin{Bmatrix} F_{Ax} \\ F_{Ay} \\ T_{A\theta} \end{Bmatrix} \quad (2.3)$$

$$\begin{Bmatrix} \ddot{x}_B \\ \ddot{y}_B \\ \ddot{\theta}_B \end{Bmatrix} + \frac{p_2}{p_1} \begin{bmatrix} 2\zeta_{Bx} & 0 & 0 \\ 0 & 2\zeta_{By} & 0 \\ 0 & 0 & 2\zeta_{B\theta} \end{bmatrix} \begin{Bmatrix} \dot{x}_B - \frac{1}{p_1} \cos \frac{t}{p_1} \\ \dot{y}_B \\ \dot{\theta}_B \end{Bmatrix} + \begin{bmatrix} \left(\frac{p_2}{p_1}\right)^2 & & \\ & \left(\frac{p_2}{p_1}\right)^2 & e_{By} \left(\frac{p_2}{p_1}\right)^2 \\ e_{By} \left(\frac{p_2}{p_1}\right)^2 \frac{m_B}{I_B} & -e_{Bx} \left(\frac{p_2}{p_1}\right)^2 \frac{m_B}{I_B} & \left(\frac{p_4}{p_1}\right)^2 \end{bmatrix} \begin{Bmatrix} x_B - \sin \frac{t}{p_1} + \Delta_B \\ y_B - e_{By} \\ \theta_B \end{Bmatrix} = m \begin{Bmatrix} F_{Bx} \\ F_{By} \\ T_{B\theta} \end{Bmatrix} \quad (2.4)$$

where $e_{ix} = e'_{ix} / A_g$, $e_{iy} = e'_{iy} / A_g$, $\Delta_i = \Delta'_i / A_g$, $I_i = I'_i / A_g^2$, $a = a' / A_g$, $l = l' / A_g$, $w = w' / A_g$, $p_1 = T / T_{Ax} = \omega_{Ax} / \omega$, $p_2 = T / T_{Bx} = \omega_{Bx} / \omega$, $p_3 = T / T_{A\theta} = \omega_{A\theta} / \omega$, $p_4 = T / T_{B\theta} = \omega_{B\theta} / \omega$, T is the period of the ground motion (i.e. $T = 2\pi / \omega$), $\omega_{ix}^2 = 4k / m_i$, $\omega_{i\theta}^2 = [I_i'^2 + w_i'^2 + 4(e_{ix}'^2 + e_{iy}'^2)]k / I_i'$, $\zeta_{ix} = c_i / (2m_i\omega_{ix})$, $\zeta_{i\theta} = c_i' / (2I_i'\omega_{i\theta})$ ($i = A, B$), and $m = m_A / m_B$ is the mass ratio between the two towers. Since the two towers are assumed to have identical lateral stiffness (i.e. $K_A = K_B = 4k$), recalling $\omega_{ix}^2 = K_i / m_i$, we have $m = (\omega_{Bx} / \omega_{Ax})^2 = (p_2 / p_1)^2$. The impact forces have been normalized as $F_{ix} = F'_{ix} / (A_g k_{Ax})$ and $F_{iy} = F'_{iy} / (A_g k_{Ax})$, and the impact torques have been normalized as $T_{i\theta} = T'_{i\theta} / (k_{Ax} I_i / m_i)$ ($i = A, B$).

2.2 Impact Forces

Following the models of Davis (1992) and Chau and Wei (2001), the pounding force is modeled utilizing the Hertz contact law as:

$$F = \begin{cases} \beta \cdot d^\chi & \text{for } d > 0 \\ 0 & \text{for } d \leq 0 \end{cases} \quad (2.5)$$

where d is the normalized penetration depth at the pounding point, $d = d' / A_g$, β is the normalized impact stiffness parameter, $\beta = \beta' / (k_{Ax} A_g^{1-\chi})$, which is a function of the elastic properties and geometry of the two contact bodies (Goldsmith 1960), and χ is the contact force exponent, with $\chi = 1.5$ corresponding to the Hertz contact law, and $\chi = 1$ representing linear contact.

Note that for torsional pounding, impacts do not necessarily occur between neighboring corners of the two towers. In our calculations, the relative locations of the two towers are checked at every time step to determine whether pounding occurs or not. Once any pounding occurs, the locations of the impact and consequently the penetration depth d are determined. Then the impact forces and torques on each tower are calculated. To be more complex than translational pounding, there are totally thirteen different cases of torsional pounding between the two towers. The details will not be given here and can be referred in Wang (2008).

2.3 Method of Solution

After the impact forces and torques are determined, the torsional pounding between the two towers can be solved through Eqns. 2.3 and 2.4, which comprise of six coupled second-order differential equations. Numerical integration is used here to solve the system of differential equations. First we define the following vector:

$$\underline{\mathbf{y}} = \{x_A \quad \dot{x}_A \quad y_A \quad \dot{y}_A \quad \theta_A \quad \dot{\theta}_A \quad x_B \quad \dot{x}_B \quad y_B \quad \dot{y}_B \quad \theta_B \quad \dot{\theta}_B\}' \quad (2.6)$$

where the symbol $'$ means transpose of vector. Then Eqns. 2.3 and 2.4 are rewritten as a set of 12 first-order differential equations as $\dot{\underline{\mathbf{y}}} = f(t, \underline{\mathbf{y}})$, with a initial value of $\underline{\mathbf{y}}(t_0) = \underline{\mathbf{y}}_0$ representing the initial displacements and velocities of the two towers. Finally this set of differential equations is numerically solved using the fourth-order Runge-Kutta method with an adaptive step size control (Press et al. 1992). The allowable error in the iterations was set to 0.1%. The initial time step was set by the program automatically, typically in the order of 0.01, but this change with the current values of the first derivatives of the displacement variables.

To search for continuous impacts (i.e. non-transient impacts), the approach used by Davis (1992) and Chau and

Wei (2001) is adopted here. In particular, the numerical integrations are first performed for 40 excitation cycles and all impacts occurred in the next 8 cycles are reported. Through extensive numerical simulations, we found this approach also appears to be reasonable for our problem of torsional pounding.

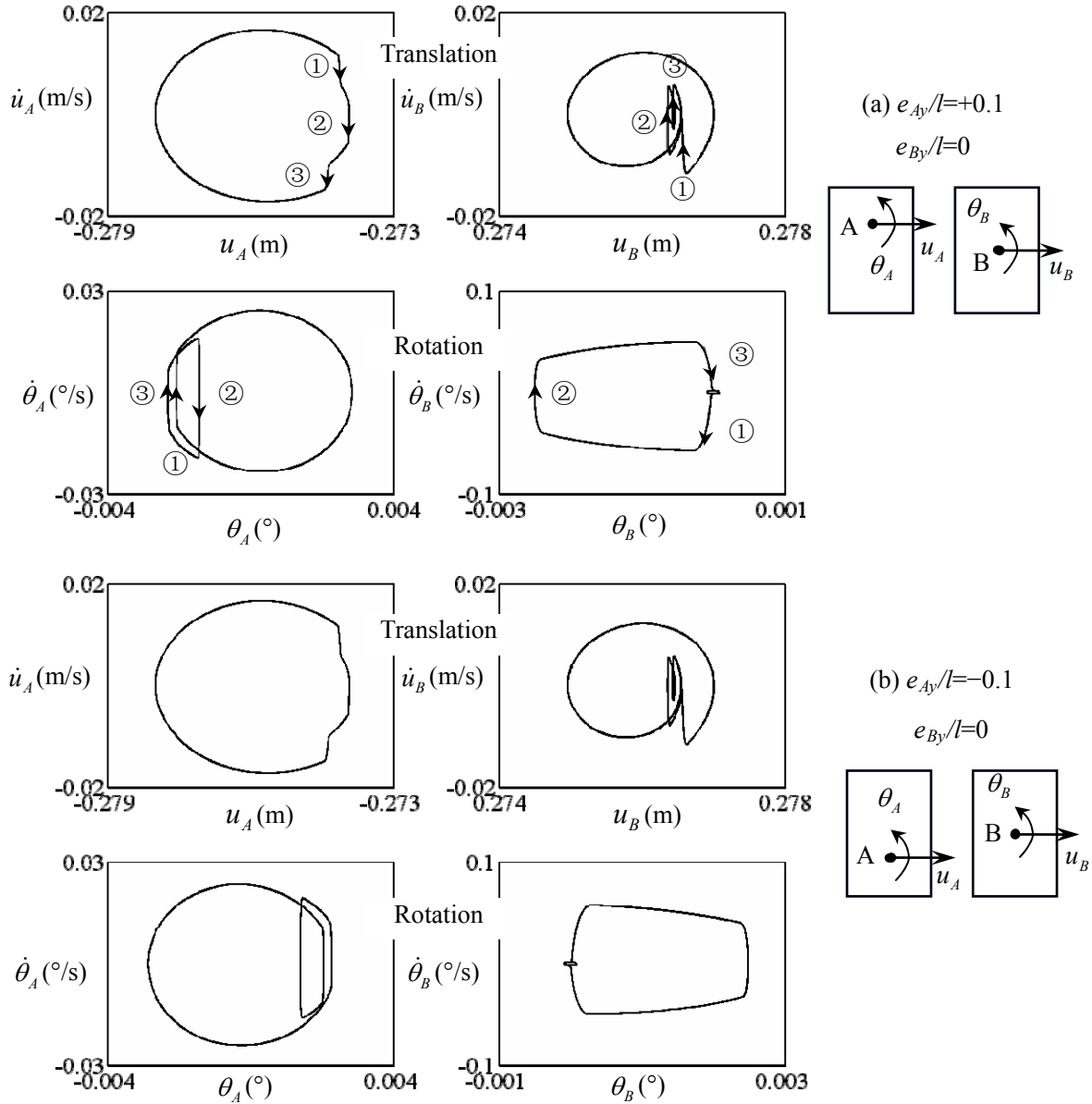


Figure 3 Validation of the solving method by comparing the steady pounding phase diagrams when the Tower A has opposite eccentricities: (a) $e_{Ay}/l = +0.1$; (b) $e_{Ay}/l = -0.1$. Other parameters are $e_{By}/l = 0$, $T/T_{Ax} = 0.7$,

$$T_{Ax}/T_{Bx} = 1.5, \quad \zeta_{Ax} = \zeta_{Bx} = 0.03, \quad \zeta_{A\theta} = \zeta_{B\theta} = 0.03 \text{ and } a = 1.0.$$

2.4 Validation of Solving Method

The solving method was validated before torsional pounding phenomena are discussed. For translation pounding, the results given by the present method have been compared with the results published by Davis (1992) and Chau and Wei (2001), and they gave nearly the same results. For torsional pounding, the method was further validated through the following way: setting the normalized eccentricity of Tower A (e_{Ay}/l) to be +0.1 and -0.1 respectively while keeping the other parameters all the same ($e_{By}/l = 0$, $T/T_{Ax} = 0.7$, $T_{Ax}/T_{Bx} = 1.5$,

$\zeta_{Ax} = \zeta_{Bx} = 0.03$, $\zeta_{A\theta} = \zeta_{B\theta} = 0.03$ and $a = 1.0$), and comparing the resulting steady pounding phase diagrams. As shown in Figure 3, when the eccentricity of Tower A is changed from +0.1 and -0.1, the translational phase diagrams at the CMs of the two towers remain unchanged whereas the rotation phase diagrams change to be opposite. The results are considered to be reasonable, suggesting the method used in this study is valid.

3. RESULTS AND DISCUSSIONS

A large number of numerical simulations have been carried out to investigate the effects of various parameters, such as the excitation frequency, damping ratio, separation distance and eccentricity, on torsional pounding. But due to space limitation, only a minor part of the results will be discussed here. The details can be referred in Wang (2008).

3.1 Chaotic Impacts

Figure 4 plots the normalized relative impact velocity $V/(A_g \omega_{Ax})$ versus the normalized excitation period T/T_{Ax} for $T_{Ax}/T_{Bx} = 1.5$, $\zeta_{Ax} = \zeta_{Bx} = 0.03$, $\zeta_{A\theta} = \zeta_{B\theta} = 0.03$, $w/l = 0.55$ and $a = 1.0$. In the figure, Tower A is set to be asymmetric (i.e. $e_{Ay}/l = 0.1$) and Tower B to be symmetric (i.e. $e_{By}/l = 0.0$). The contact force exponent is set as $\chi = 3/2$ representing Hertz contact, and the impact stiffness is set as $\beta = 1000$ representing a relatively stiff contact (Davis, 1992). Recalling $m = m_A/m_B$ and $m = (\omega_{Bx}/\omega_{Ax})^2 = (T_{Ax}/T_{Bx})^2$, we get $m_A/m_B = 2.25$, which means Tower A is more massive than Tower B. Each cross in the figure represents an impact. The impact velocity spectrum for translational pounding when $e_{Ay}/l = 0.0$ [i.e. Figure 5 in Chau and Wei (2001)] is also plotted by dots for comparison.

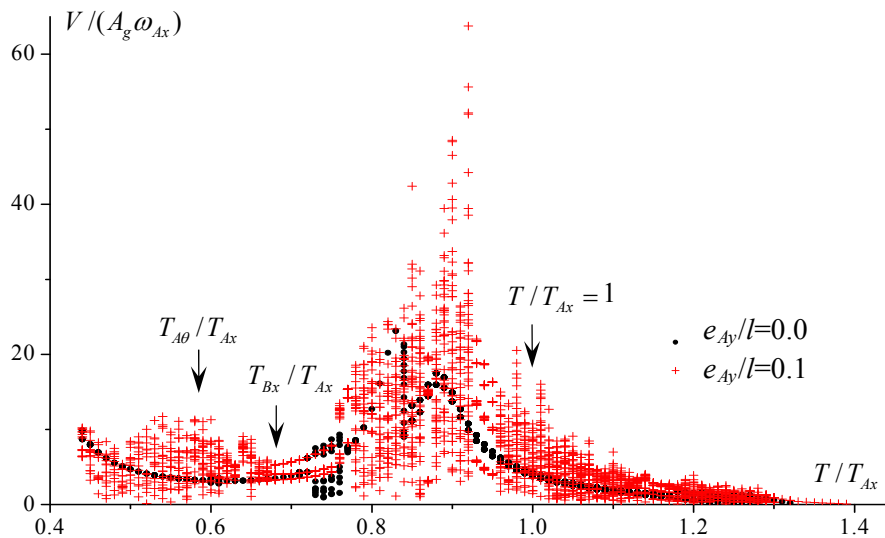


Figure 4 Comparison of relative impact velocity spectra versus T/T_{Ax} for torsional ($e_{Ay}/l = 0.1$, denoted by crosses) and translation ($e_{Ay}/l = 0.0$, denoted by dots) poundings

It is seen that the impact velocity spectra for translational and torsional poundings have similar shapes. But major differences still exist. For translational pounding, chaotic impacts only occur at limited excitation periods and most of the impacts are periodic. But for torsional pounding, most of the impacts are chaotic. For these chaotic impacts, the recorded impact velocities within eight excitation cycles appear to be quite scattered. In addition, the maximum impact velocity of torsional pounding is almost three times of that of translational

pounding. All of these suggest that torsional pounding is more complex and severer than translational pounding.

3.2 Group Periodic Impacts

The other difference is that group periodic impacts were observed for the first time for the case of torsional pounding (e.g. $T/T_{Ax} = 0.68-0.77, 0.87, 0.93-0.95$ and $1.3-1.39$ in Figure 4) but not in translational pounding. The group periodic impacts mean a group of non-periodic impacts repeating themselves periodically, and are a unique pounding phenomenon first observed in shaking table tests by Chau et al. (2003). An example of group periodic impacts has been shown in Figure 3(a) when $T/T_{Ax} = 0.70$. For this case, there are three impacts within one excitation cycle, occurring at the Corners C, F and C in sequential order. The location of each impact (labeled as ①-③) in the phase diagrams is indicated. These three impacts are clearly shown by the sudden jumps in both translational and rotational velocities in these phase diagrams.

3.3 Effect of Eccentricity

To investigate the effect of eccentricity, Figure 5 compares the relative impact velocity spectrum for $e_{Ay}/l = 0.2$ to that of Figure 4 for $e_{Ay}/l = 0.1$. It is evident that the shape of relative impact velocity spectrum remains almost unchanged, while the maximum velocity drops about 20%. But at some excitation periods (such as those periods near $T_{A\theta}$ and T_{Bx}), the maximum impact velocities increase with the value of eccentricity. But, as a whole, the impact velocity spectrum does not change significantly by the doubling of eccentricity.

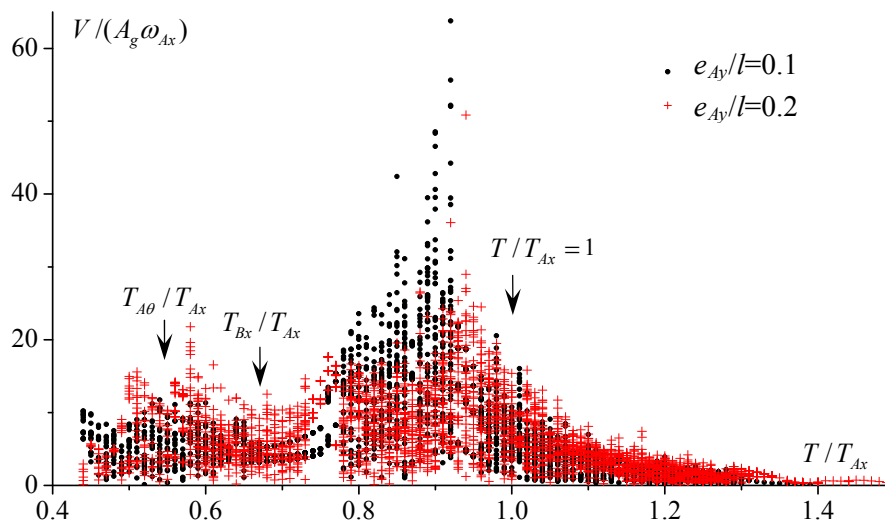


Figure 5 Comparison of relative impact velocity spectra for $e_{Ay}/l = 0.1$ and 0.2

4. CONCLUSIONS

In this paper, the torsional pounding between two asymmetric single-story towers was modeled using the nonlinear Hertz contact law. Numerical simulation results show that generally torsional impacts tend to be much more complex than translational pounding, and most of them are either chaotic or group periodic. Chaotic impacts may result in quite scattered impact velocities, and thus make the torsional pounding even more unpredictable. The group periodic pounding observed in shaking table tests by Chau et al. (2003) was simulated and replicated numerically for the first time by incorporating torsional responses, which cannot be explained

through numerical simulations for translational poundings alone. The impact velocity spectrum is not affected significantly by the doubling of eccentricity. Although the present model is highly idealized comparing to actual asymmetric multi-story structures, we believe that the present results can capture the essence of nonlinear seismic torsional pounding phenomenon with the minimum number of parameters involved. The results of this study should provide valuable insights into this unknown domain of seismic torsional pounding.

Acknowledgements: This work is fully supported by Research Grants Council of the Hong Kong Special Administrative Region, China through Project No. PolyU 5035/02E.

REFERENCES

- Anagnostopoulos, S.A. (1988). Pounding of buildings in series during earthquakes. *Earthquake Engineering and Structural Dynamics* **16**, 443-456.
- Anagnostopoulos, S.A. (1994). Earthquake induced pounding: State of the art. *Proceedings of the 10th European Conference on Earthquake Engineering, Vienna, Austria* **2**, 897-905.
- Chau, K.T. and Wei, X.X. (2001). Pounding of structures modeled as nonlinear impacts of two oscillators. *Earthquake Engineering and Structural Dynamics* **30**, 633-651.
- Chau, K.T., Wei, X.X., Guo, X. and Shen, C.Y. (2003). Experimental and theoretical simulations of seismic pounding between two adjacent structures. *Earthquake Engineering and Structural Dynamics* **32**, 537-554.
- Davis, R.O. (1992). Pounding of buildings modeled by an impact oscillator. *Earthquake Engineering and Structural Dynamics* **21**, 253-274.
- Goldsmith, W. (1960). Impact, Edward Arnold, London, UK.
- Gong, L. and Hao, H. (2005). Analysis of coupled lateral-torsional-pounding responses of one-storey asymmetric adjacent structures subjected to bi-directional ground motions Part I: Uniform ground motion input. *Advances in Structural Engineering* **8: 5**, 463-479.
- Jankowski, R. (2005). Non-linear viscoelastic modeling of earthquake-induced structural pounding. *Earthquake Engineering and Structural Dynamics* **34**, 595-611.
- Jing, H.S. and Young, M.H. (1991). Impact interactions between two vibration systems under random excitation. *Earthquake Engineering and Structural Dynamics* **20**, 667-681.
- Kasai, K. and Maison, B.F. (1997). Building pounding damage during the 1989 Loma Prieta Earthquake. *Engineering Structures* **19**: 195-207.
- Leibovich, E., Rutenberg, A. and Yankelevsky, D.Z. (1996). On eccentric seismic pounding of symmetric buildings. *Earthquake Engineering and Structural Dynamics* **25**, 219-233.
- Liu, D.H., Yang, C.R. and Zhong, X.G. (1993). Seismic Design of Tall Buildings, China Architecture & Building Press, Beijing, China (in Chinese).
- Miller, R.K. (1980). Steady vibroimpact at a seismic joint between adjacent structures. *Proceedings of the 7th World Conference of Earthquake Engineering, Istanbul, Turkey* **6**, 57-64.
- Mouzakis, H. and Papadrakakis, M. (2004). Three dimensional nonlinear building pounding with friction during earthquakes. *Journal of Earthquake Engineering* **8: 1**, 107-132.
- Muthukumar, S. and DesRoches, R. (2006). A Hertz contact model with non-linear damping for pounding simulation. *Earthquake Engineering and Structural Dynamics* **35**, 811-828.
- Naeim, F., Lew, M., Huang, S.C., Lam, H.K. and Carpenter, L.D. (2000). The performance of tall buildings during the 21 September 1999 Chi-Chi earthquake, Taiwan. *The Structural Design of Tall Buildings* **9**, 137-160.
- Papadrakakis, M., Apostolopoulou, C., Zacharopoulos, A. and Bitzarakis, S. (1996). Three-dimensional simulation of structural pounding during earthquakes. *Journal of Engineering Mechanics, ASCE* **122**, 423-431.
- Rosenblueth, E. and Meli, R. (1986). The 1985 earthquake: causes and effects in Mexico City. *Concrete International, American Concrete Institute* **8: 5**, 23-34.
- Wakabayashi, M. (1986). Design of Earthquake-Resistant Buildings, McGraw-Hill, Inc., USA.
- Wang, L.X. (2008). Seismic vulnerability and pounding hazard of asymmetric buildings with transfer system: experimental and analytical modeling, Ph.D. thesis, Hong Kong Polytechnic University.